

Chapter 7

Detection of Built-Up Areas in SAR Images

This chapter discusses the detection of built-up areas in high-resolution SAR images. By built-up areas we mean *areas covered by buildings*. This can be small groups of buildings, settlements or urban areas. The purpose here is thus not to detect isolated houses.

The detection of such areas is not only interesting for the automatic registration with maps or other images [65] but also for applications such as the study of the population density, the study of risks, planning of road networks, surveillance of the urban pressure on rural regions,... which all need an up-to-date overview of the location and the extent of the built-up areas.

The fastest and cheapest way to obtain these updates is by extracting the information automatically from remotely sensed data. Many papers describing the detection of built-up areas on visual or infrared satellite images (e.g. SPOT) have been published (see [66] for a review). At this moment, the most dramatic changes in the demographical situation occur in sub-tropical and tropical regions (mainly in Africa and Asia) where the climate (clouds) makes it difficult to use optical imagery for remote sensing applications.

Although SAR thus seems to be important for the detection of built-up areas, publications on the subject are very sparse. Some recent publications focus on the detection and reconstruction of individual buildings by means of very high-resolution (0.3 - 0.5 m), interferometric and/or multi-view SAR images [67, 68, 69].

In [70] C. Gouinaud does propose a method to detect agglomerations in low-resolution multi-look SAR images (ERS1). His method is based on the combination of statistical features. He shows that classical first order statistical features (variance,skewness,...) could be interesting but that they can not be used in low-resolution images. The reason is that they can only be estimated accurately enough using a very large number of pixels. Gouinaud [70] has developed various statistical features, based on the histogram, which allow to capture the particular effect of built-up areas on the statistics of SAR images.

The method proposed in this chapter investigates the statistical and polarimetric properties of built-up areas in high-resolution SAR images and translates these properties into features that can be easily determined and which allow to high-light the presence of built-up areas. The detector combines these features.

Fig. 7.1 presents an overview of the method proposed in this chapter for the detection

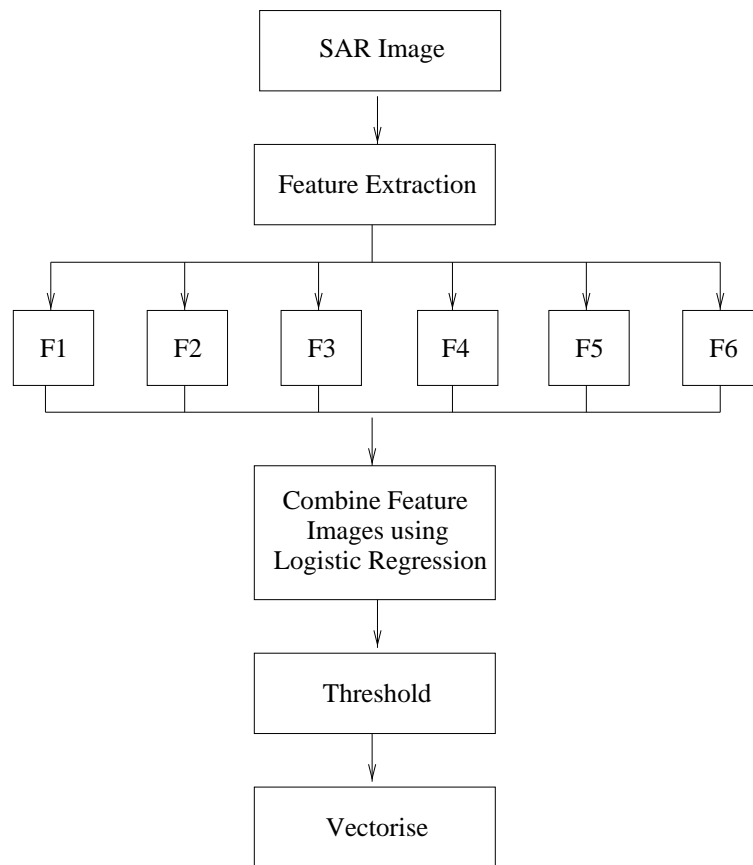


Figure 7.1: Overview of the method used for the detection of built-up areas

of built-up areas.

The method uses various features obtained either directly from the SAR images or after performing a region segmentation (MUM) discussed before (see set 6.1). These features are fused using logistic regression in order to obtain the conditional probability that a pixel (x, y) belongs to a built-up area given the set of features \mathbf{F} at that pixel. Applying a threshold to this probability map results in a pixel-wise detector for built-up areas. The final result is reached by vectorising the resulting regions that satisfy geometrical constraints.

The next section of this chapter briefly discusses some important radiometric and polarimetric properties of built-up areas in SAR images. Then the different features and the logistic regression are explained. In the last part of the chapter the results are discussed.

7.1 Radiometric and Polarimetric Characteristics of Built-Up Areas in SAR Images

The radar backscattering from built-up areas is characterised by a high degree of variation. This is due to the variation of building materials that are used as well as the occurrence of

many different scattering mechanisms within built-up areas. Fig. 7.2 presents an overview of the different types of scattering mechanisms that are encountered in built-up areas. The deterministic scatterers (dihedrals and trihedrals) found in villages [70] produce very bright reflections. Specular reflection from roofs with a slope perpendicular to the viewing angle of the radar also cause very bright reflections. On the other hand shadows or specular reflections from horizontal surfaces produce very dark regions in the image. If the radar wave gets trapped in a narrow street, multiple double-bounce scattering can occur between the walls of the buildings and the ground. The presence of vegetation between buildings (lawns, parks,...) can cause rough surface scattering or, when the scattered wave falls on the wall of a building anisotropic double bounce reflections.

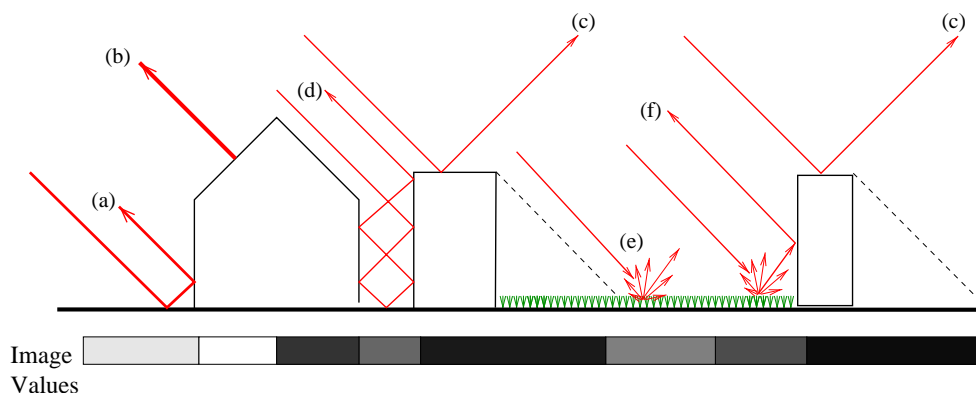


Figure 7.2: Examples of scattering mechanisms encountered in built-up areas: (a) Isotropic double-bounce, (b) Cooperative specular reflection, (c) Non-cooperative specular reflection, (d) Multiple double-bounce, (e) Rough surface scattering, (f) Anisotropic double-bounce.

These effects cause the statistical distribution of the image values to differ highly from the distribution found in uniform regions. Another important aspect is the difference in correlation between the different polarisations found in vegetated areas and built-up areas. In vegetated areas the correlation between co-polarised and cross-polarised component images (i.e. between HH/HV or VV/HV) is negligible [71]. In villages, mainly the presence of the deterministic scatterers produces a much higher correlation between cross-polarised components. The amplitudes of the correlations between HH/HV and VV/HV approaches the one found between HH and VV. This was already observed in section 4.2.3 where examples of the inter-channel correlation coefficient for various types of landcovers were presented in table 4.4.

The features we used for the detection of agglomerations are based on these properties.

7.2 Description of the Features

The first three features that were used for the detection of built-up areas are based on the fact that the SAR image is not uniform in such areas. In many ways the statistics of built-up areas are different from those of uniform regions. The last three features are

based on the correlation between the co- and cross-polarised component images. Most features are calculated in rectangular windows scanning the image. Only the first feature is calculated using the uniform regions found by the image segmentation method discussed in chapter 6.

7.2.1 Distance Measure

This feature is based on the regions that were found by the image segmentation using the MUM method based on the Mahalanobis distance (see sect. 6.1.3). The result of this method using the 0.5 % false alarm threshold is presented in fig 7.3 (left). On the right in the same figure a part, manually warped to image coordinates, is shown as a reference. The unusual high threshold used in the segmentation causes an over-segmented image, but this is well-suited for the distance measure defined below.

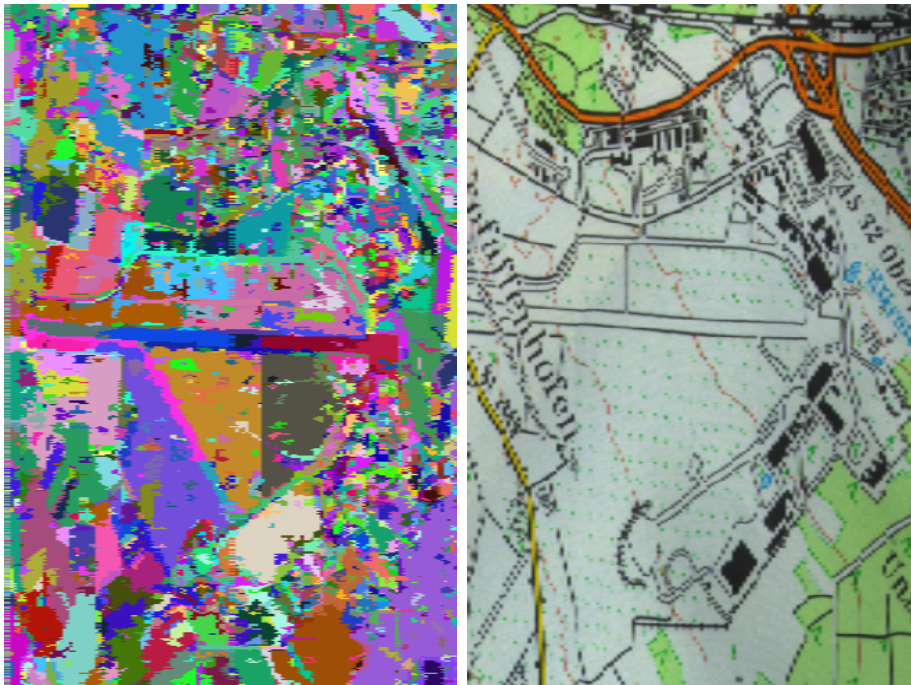


Figure 7.3: Result of MUM (left) and corresponding map (right)

The idea is that in a built-up area the uniform regions will be much smaller than in other parts of the image. However, this is also true for the edges between uniform regions. Hence the idea of linking a notion of isotropy to a measurement of region size. For each region its geometric centre is determined. From a geometric centre of one region, the closest centre to another region is determined along different directions. In practice the space around the current centre is subdivided into 8 parts (each corresponding to 45 degree) and in each part the smallest distance is kept. The “distance” feature is the next largest of these smallest distances (see fig. 7.4).

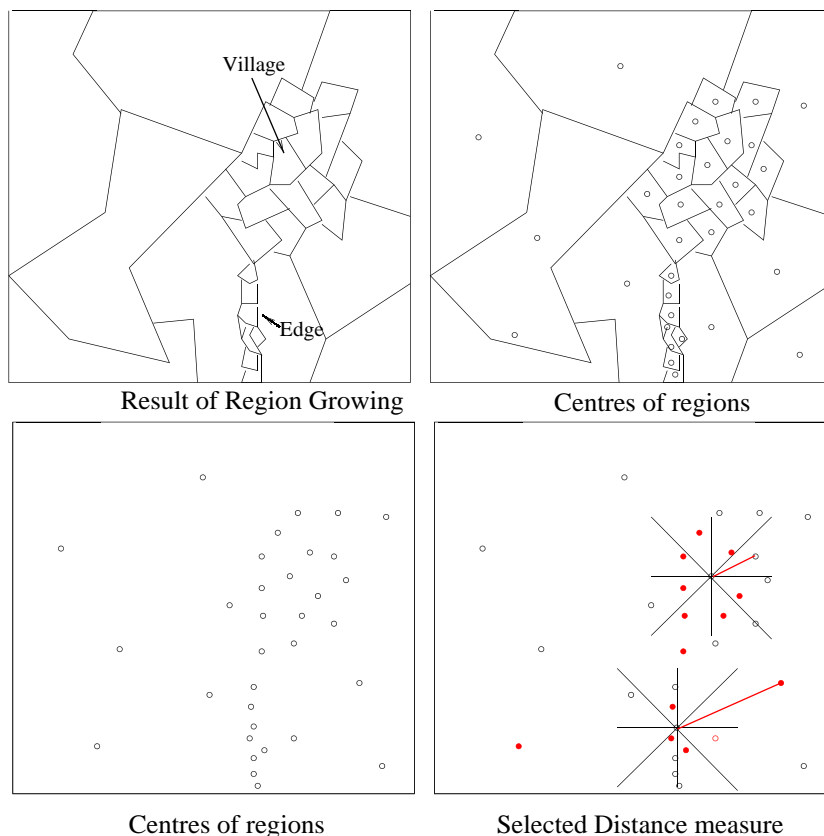


Figure 7.4: Definition of the distance measure

This is feature F_1 . The smaller this distance, the more likely the region belongs to a built-up area. This procedure eliminates the problem of edges between uniform regions as for these types of regions the distance will only be small in a few directions.

7.2.2 Skewness Measure

In uniform regions the amplitude image follows a Raleigh distribution which is skewed to the left. In built-up areas the distribution becomes more symmetric and can even be skewed to the right because of the presence of bright spots or bright lines. However, using the classical definition of skewness results in a patch pattern in the skewness image. The main reason is that a few isolated very bright spots have a very large influence on these estimators yielding results that are unstable.

We used an estimator of the skewness based on the median and two percentiles that are symmetrical around the median (P_t and P_{1-t} with $0.0 \leq t < 0.5$) of the local pixel-value distribution:

$$F_2 = \frac{(P_{1-t} - P_{0.50}) - (P_{0.50} - P_t)}{P_{1-t} - P_t}. \quad (7.1)$$

To illustrate the problem with the classically defined skewness in agglomerations we calculated a skewness image for a small part of the SAR amplitude image using the classical

definition and the one based on percentiles (with $t=0.1$ and a 20×20 window size). In fig 7.5 can be seen that isolated bright spots cause a patch pattern in the skewness value when the classical definition is used.

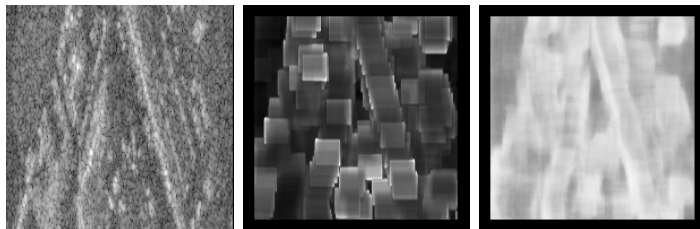


Figure 7.5: Part of original image (left), classical skewness (centre), skewness based on percentiles (right)

7.2.3 Variance Measure

For uniform regions the variance is solely due to the speckle. This variance is very low in the log-intensity image (and equal to a constant independent of the region [10]). In regions containing a lot of deterministic scatterers, the variance becomes much higher. We defined a measure of the variance, or rather of the lack of variance, analogously to the definition of the skewness:

$$F_3 = \frac{P_{0.75} - P_{0.25}}{P_{0.90} - P_{0.10}}. \quad (7.2)$$

Another advantage of this measure is the fact that it is bounded like the other proposed statistical parameters which would not be the case for the classically defined variance.

7.2.4 Interchannel Correlation

In uniform regions with azimuthal symmetry (most vegetation) the correlation between co-polarised and cross-polarised component images, i.e. between the HH and HV image at one hand and the VV and HV image at the other hand, is very low [59, 71]. In areas with a lot of deterministic scatterers, such as dihedrals and trihedrals (e.g. in villages but also at the edges of forests) this correlation increases up to a level comparable to that of the correlation between co-polarised components (HH/VV). Therefore we also used these three inter-channel correlations as features:

$$F_4 = \rho_{HH/HV} = \frac{|\langle S_{HH} S_{HV}^* \rangle|}{\sqrt{\langle |S_{HH}|^2 \rangle \langle |S_{HV}|^2 \rangle}}, \quad (7.3)$$

$$F_5 = \rho_{VV/HV} = \frac{|\langle S_{VV} S_{HV}^* \rangle|}{\sqrt{\langle |S_{VV}|^2 \rangle \langle |S_{HV}|^2 \rangle}}, \quad (7.4)$$

$$F_6 = \rho_{HH/VV} = \frac{|\langle S_{HH} S_{VV}^* \rangle|}{\sqrt{\langle |S_{HH}|^2 \rangle \langle |S_{VV}|^2 \rangle}}. \quad (7.5)$$

Note that these three features correspond to the norm of the normalised off-diagonal elements of the polarimetric covariance matrix and as such represent an important part of the polarimetric information contained in the polarimetric image.

7.2.5 Overview of Feature Images

Calculating the different features in each pixel of the original image yields feature images. Fig. 7.6 shows the original SAR image together with the corresponding region of a map that was transformed into the coordinate space of the SAR image. Fig. 7.7 to fig. 7.9 shows the different feature images. The statistical parameters were calculated in a 40×40 window scanning the image except for the skewness that was calculated in a 20×20 window. All features were calculated using the log-intensity image except for the skewness which was calculated on the amplitude image. The figures show that the different features are complementary. Most of the features show the villages either as bright or dark regions. False targets consist mainly of edges between fields and forests. In the “distance image” the edges do not cause false targets. We now need to find a way to combine the different features in order to obtain a good detection of agglomerations.

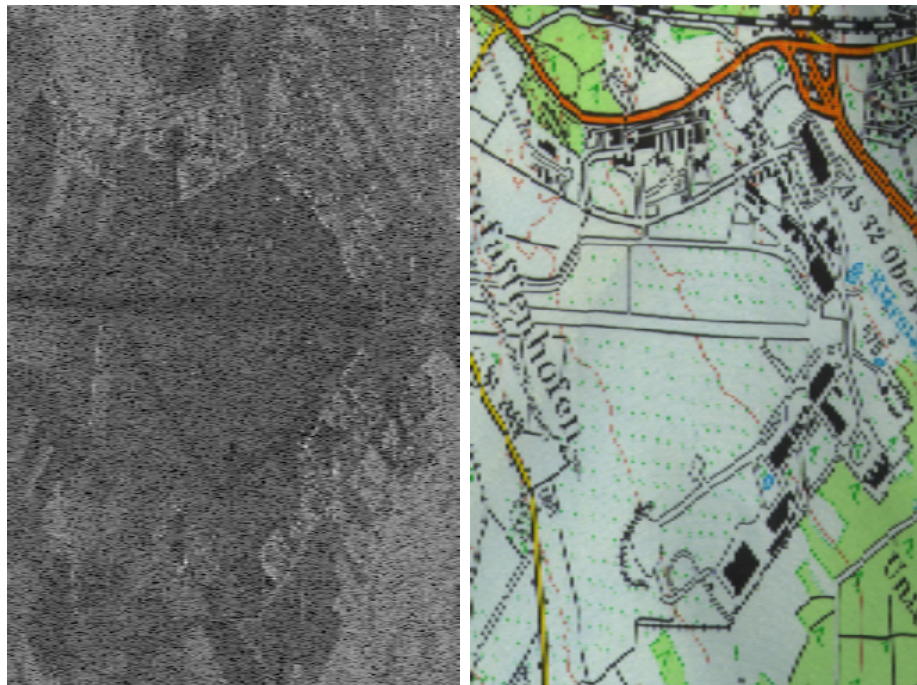


Figure 7.6: Original image (HH polarisation) and corresponding map

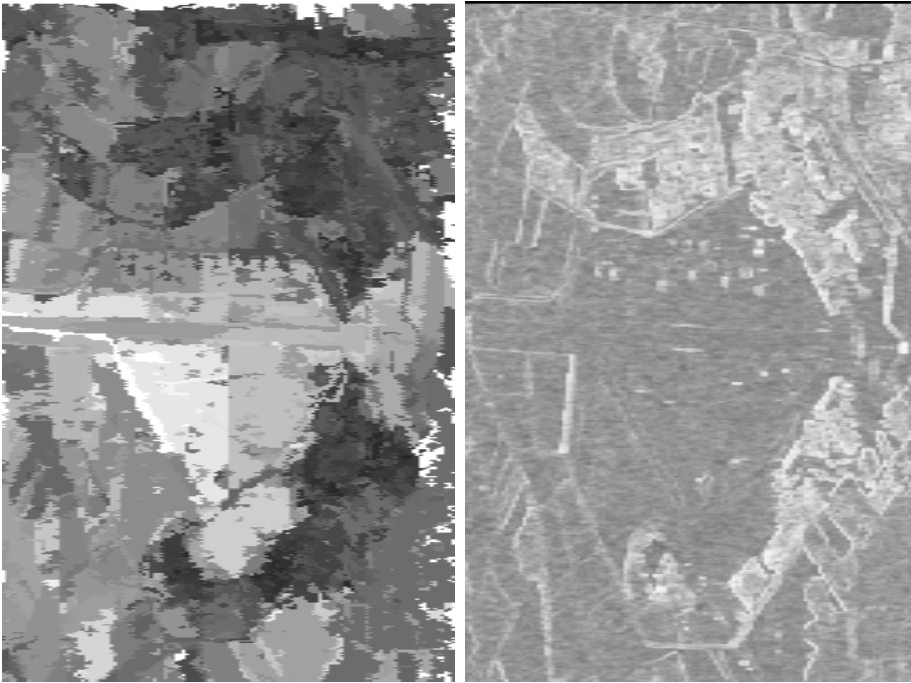


Figure 7.7: Distance and skewness measures

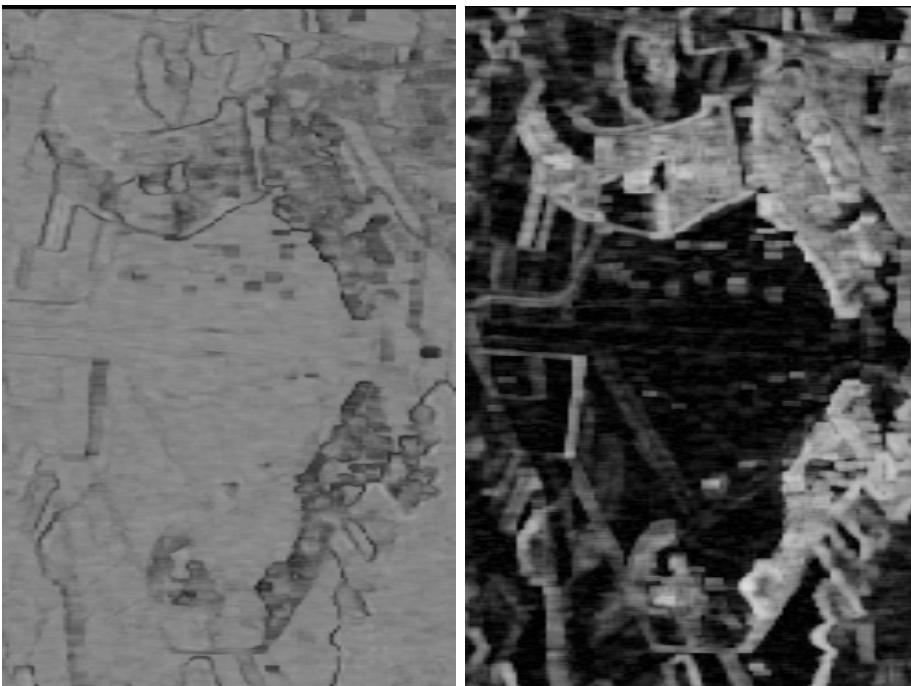
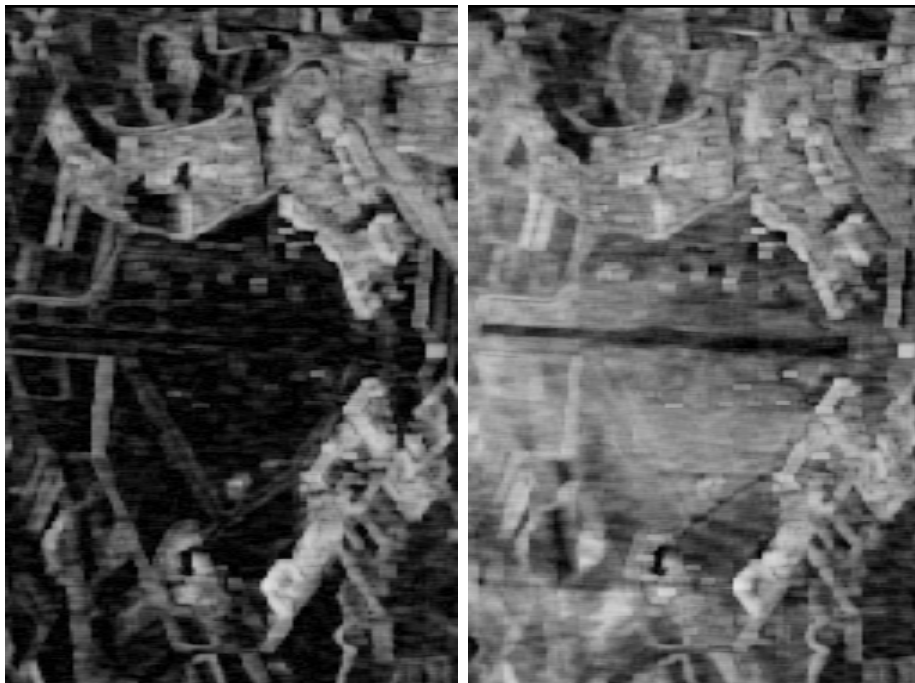


Figure 7.8: Variance measure and $\rho_{HH/HV}$

Figure 7.9: $\rho_{VV/HV}$ and $\rho_{HH/VV}$

7.3 Feature Fusion using Logistic Regression

Logistic regression [72] offers a way to combine the different features while at the same time yielding a measure of their respective discriminative power. It is a supervised approach: In the 1200×10000 single-look image we identified a priori 1000 target (built-up areas) and 1000 background pixels to constitute the learning set. In the learning phase, at each pixel of the learning set, the different features were calculated and each set of features was labeled as belonging to the built-up area (1) or not (0).

Logistic regression is then used to find a combination of the form :

$$p_{xy}(target | \mathbf{F}) = \frac{e^{b_0 + \sum_i b_i F_i(x,y)}}{1 + e^{b_0 + \sum_i b_i F_i(x,y)}}, \quad (7.6)$$

in which $p_{xy}(target | \mathbf{F})$ is the conditional probability that a pixel (x, y) belongs to the class 1 given the vector of features \mathbf{F} at the given pixel.

The logistic regression was carried out using Wald's forward method. In this method, at each step, the most discriminant feature is added and the significance of adding it to the model is verified. This means that not all features will necessarily be included into the model. The Wald coefficient is a measure for the significance of the feature, i.e. its discriminative power for the given task. Table 7.1 shows the weights resulting from the logistic regression as well as the Wald coefficients.

Apparently all features were selected. This supports the idea that they represent complementary information. The values of the Wald coefficient show that the most significant

Name	Parameter Name	Weight	Wald
F_1	Distance	-0.0401	159
F_2	Skewness	0.0229	31.9
F_3	VarMeas	-0.0197	24.09
F_4	$\rho_{HH/HV}$	0.0140	6.24
F_5	$\rho_{VV/HV}$	0.0482	76.3
F_6	$\rho_{HH/VV}$	-0.0326	53.4
F_0	Constant	0.0112	0.0001

Table 7.1: Results of logistic regression for the complete feature set

features are the distance and two of the correlations ($\rho_{VV/HV}$ and $\rho_{HH/VV}$). The least significant (although still having non-zero weight) is the correlation $\rho_{HH/HV}$. This is not surprising because it is highly correlated with $\rho_{VV/HV}$ and the VV-polarised image presents more detail.

Table 7.2 shows the results of the logistic regression found when the polarimetric information is not used. In this case the distance measure and the skewness are the most important parameters. The weights obtained when the distance measure is left out of the feature set are presented in table 7.3.

Name	Parameter Name	Weight	Wald
F_1	Distance	-0.048	275
F_2	Skewness	0.052	160
F_3	VarMeas	-0.033	41
F_0	Constant	-0.290	0.067

Table 7.2: Results of logistic regression when the polarimetric features are left out

Name	Parameter Name	Weight	Wald
F_2	Skewness	0.027	34
F_3	VarMeas	-0.019	12
F_4	$\rho_{HH/HV}$	0.010	3.9
F_5	$\rho_{VV/HV}$	0.058	125
F_6	$\rho_{HH/VV}$	-0.032	67
F_0	Constant	-5.328	22

Table 7.3: Results of logistic regression when the distance measure is left out

7.4 Results of the Pixel-Wise Detector of Built-Up Areas

Applying the weights found on the learning set to the complete feature image set gives the result shown in fig. 7.10. If a threshold of 90 % is applied on the output of the logistic regression most of the built-up areas are well detected. The effect of such a threshold is shown in fig. 7.11. In the figure the results are labelled using the ground truth extracted from the map. The dark regions are false targets, the white ones are the correctly detected built-up areas, dark grey is the background and the light grey regions correspond to undetected parts of the built-up areas.



Figure 7.10: Results of the logistic regression

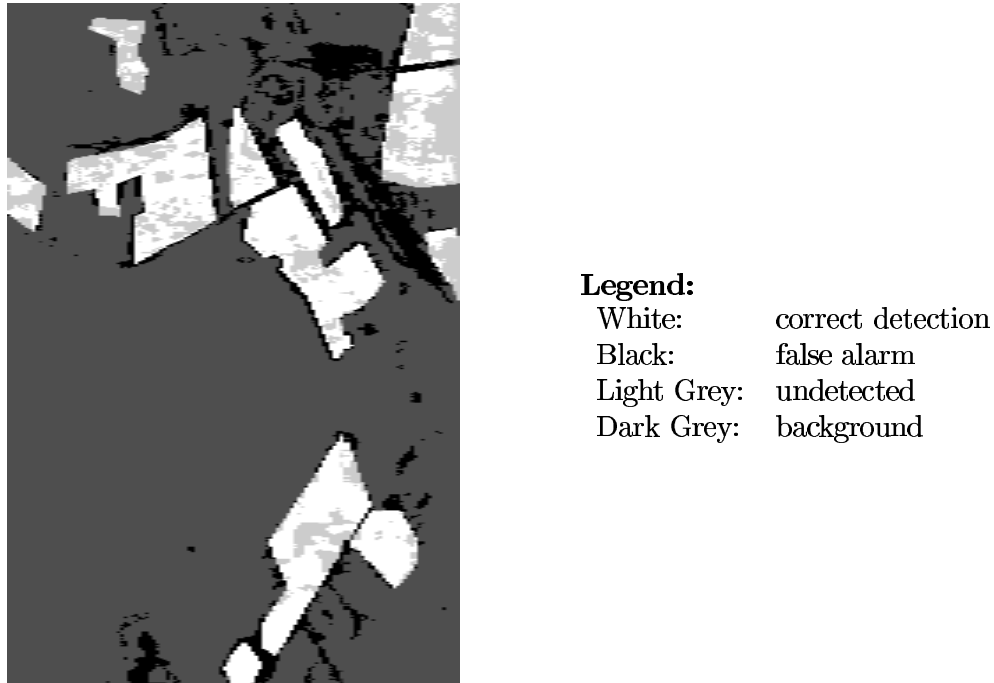


Figure 7.11: Ground truthed results at 90 % threshold

False targets are found at the position of the motorway and especially at the cross-roads of the motorway. Some small false alarms do correspond to the edges between forests and fields. The false target at the bottom left is an earthen wall. The false targets that remain are thus mainly due to regions in the image where deterministic scatterers are also likely to occur. Most of the so-called undetected parts are due to the crudeness of the ground truth, i.e. the contour of built-up areas was delimited but can still contain free spaces (fields, lawns, etc.). If one is only interested in detecting large agglomerations most false targets could be eliminated by constraining the size of the detected regions and eliminating narrow regions.

In fig. 7.12 the probability of detection is plotted against the probability of false targets. Points on this ROC curve are obtained by varying the detection threshold and for each threshold calculating the probability of detection and false alarms based on the ground truth discussed above. Both probabilities were determined on a pixel-wise basis, i.e. the probability of detection was defined as the number of correctly detected pixels divided by the number of pixels contained in the built-up areas extracted from the map and the false alarm probability is the ratio of the number of false alarm pixels to the number of pixels in the image not belonging to built-up areas.

Fig. 7.12 shows the results for the complete feature-set as well as for the reduced feature set where the distance measure and the polarimetric information are left out respectively. Although, in the full-feature set the distance measure has the highest Wald coefficient, leaving out the polarimetric information (the three inter-channel correlations) reduces performance more than leaving out the distance measure.

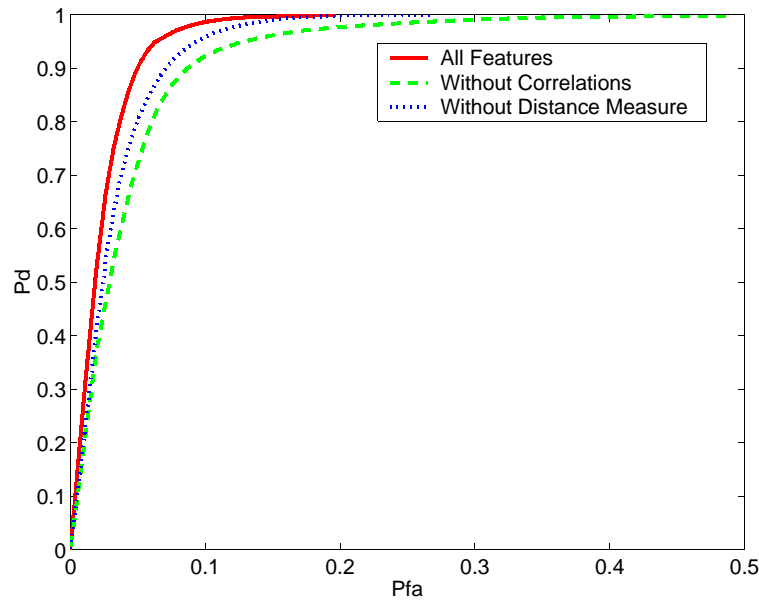


Figure 7.12: ROC curves for the detector for the full set of features, leaving out the distance measure and leaving out the inter-channel correlation

7.5 Vectorisation of the Detected Built-Up Areas

The idea is to use the detected built-up areas for registering the SAR image with a map. It is unlikely that we can detect isolated houses in the SAR image with the presented method. Hence we are only interested in finding larger built-up areas in the SAR image. As many of the false targets produced by the pixel-wise detection of built-up areas consist of isolated vertical structures or elongated man-made structures (e.g. the motorway) these can thus be eliminated using constraints on region size and aspect ratio. In order to facilitate the registration with the map, the image resulting from the logistic regression is first converted to ground range with approximately square pixels of a size similar to the pixelsize of the scanned map (i.e. a shrink of 2 in x-direction and 6 in y-direction yielding a resolution of 3 m for the SAR image compared to 4.33 m for the map). Then a threshold is applied and the size of the resulting regions is limited. An erosion (5 pixels wide) is used to eliminate thin structures and links between built-up areas. The resulting regions are vectorised as shown in figure 7.13. The red lines are the result of the vectorisation. The greyvalues are the inverse of the output of the pixel-wise detector. The left figure shows the results of applying a threshold at 80 % and limiting the region size to be larger than 5000 pixels (approx. $45000m^2$). In the figure on the right the result is shown of a threshold of 60 % and a minimal size of 2000 pixels.

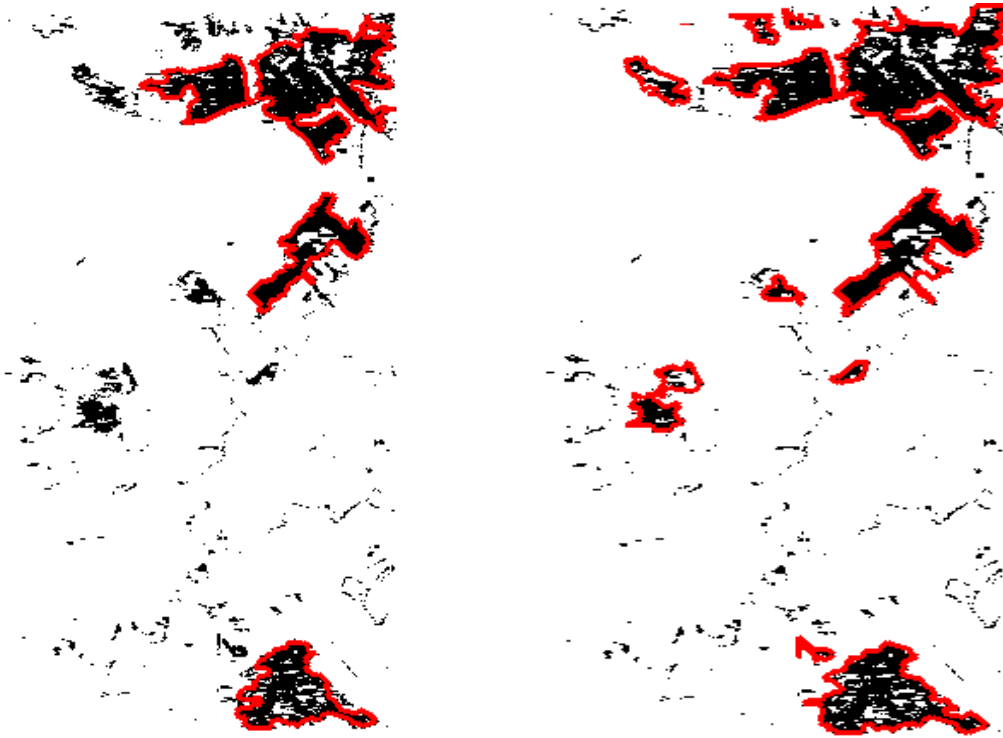


Figure 7.13: Detected built-up areas with $T=80\%$, $\text{minsize}=5000$ (left) and $T=60\%$, $\text{minsize}=2000$ (right)